J|A|C|S
ARTICLES
Published on Web 06/02/2007

Mechanism of Activation of a Hafnium Pyridyl−Amide Olefin Polymerization Catalyst: Ligand Modification by Monomer

Robert D. J. Froese,*,† Phillip D. Hustad,‡ Roger L. Kuhlman,‡ and Timothy T. Wenzel†

Contribution from The Dow Chemical Company, 1776 Building, Midland, Michigan 48674, and The Dow Chemical Company, 2301 N. Brazosport Blvd., Freeport, Texas 77541

Received January 31, 2007; E-mail: froeserd@dow.com

Abstract: We have investigated the olefin polymerization mechanism of hafnium catalysts supported by a pyridyl−amide ligand with an *ortho*-metalated naphthyl group. Ethylene−α-olefin copolymers from these catalysts have broad molecular weight distributions that can be fit to a bimodal distribution. We propose a unique mechanism to explain this behavior involving monomer modification of the catalyst, which generates multiple catalyst species when multiple monomers are present. More specifically, we present evidence that the hafnium alkyl cation initially undergoes monomer insertion into the Hf−*naphthyl* bond, which permanently modifies the ligand to generate new highly active olefin polymerization catalysts. Under ethylene/octene copolymerization conditions, a plurality of new catalysts is formed in relative proportion to the respective monomer concentrations. Due to the asymmetry of the metal complex, two "ethylene-inserted" and eight "octene-inserted" isomers are possible, but it is a useful approximation to consider only one of each in the polymerization behavior. Consequently, gel permeation chromatography data for the polymers can be fit to a bimodal distribution having a continuous shift from a predominantly low molecular weight fraction to predominantly higher molecular weight fraction as [octene]/[ethylene] is increased. Theoretical calculations show that such insertions into the Hf−aryl bond have lower barriers than corresponding insertions into the Hf−alkyl bond. The driving forces for this insertion into the Hf−aryl bond include elimination of an eclipsing H−H interaction and formation of a stabilizing Hf−arene interaction. These new "monomer-inserted catalysts" have no β-agostic interaction, very weak olefin binding, and olefin-insertion transition states which differ on the two sides by more than 4 kcal/mol. Thus, the barrier to site epimerization is very low and high polymerization rates are possible even when the chain wags prior to every insertion. Experimental evidence for aryl-insertion products is obtained from reactions of ethylene ($^{13}C_2H_4$ NMR studies) or 4-methyl-1-pentene (4M1P) using relatively low monomer/catalyst ratios. Quantitative generation of monomer-inserted products is complicated by slow initiation kinetics followed by fast polymerization kinetics. However, NMR evidence for reaction with $^{13}C_2H_4$ was observed in situ at low temperature, and the attachment of monomer to ligand was confirmed by GC/MS and ^{13}C NMR after quenching. Furthermore, a 4M1P-appended ligand was isolated from a polymerization reaction (50:1 monomer:catalyst) by column chromatography followed by multiple recrystallizations. One isomer was characterized by X-ray crystallography, which unequivocally shows a 4-methylpentyl substituent at the 2-position of the naphthyl, consistent with 1,2-insertion into the Hf−aryl bond. NMR suggests a second diastereomer (not isolated) is formed from a 1,2-insertion of opposite stereoselectivity.

Introduction

The field of olefin polymerization catalysis has grown extensively since its inception. While polymerization efficiencies first became competitive with supported Ziegler−Natta catalysts by using alumoxane cocatalysts,[1] the use of well-defined activators that generate noncoordinating or weakly coordinating anions has greatly facilitated structural elucidation of activated catalyst species[2] and detailed mechanistic studies. The ability to tailor both catalytic and polymer properties by making minor structural adjustments to these well-defined catalysts has proven to be a rich and rewarding area of research. This work has yielded catalysts with improved efficiencies and enabled synthesis of several new polyolefin architectures.[3−6]

Advances in post-metallocene catalysts[5] are not only generating improved catalysts for existing processes but also expanding the possibilities for polyolefin production. For example, py-

† The Dow Chemical Co., Midland, MI.
‡ The Dow Chemical Co., Freeport, TX.

(1) Sinn, H.; Kaminsky, W. *Adv. Organomet Chem.* **1980**, *18*, 99.
(2) (a) Jordan, R. F.; LaPointe, R. E.; Bajgur, C. S.; Echols, S. F.; Willett, R. *J. Am. Chem. Soc.* **1987**, *109*, 4111. (b) Bochmann, M.; Wilson, L. M.; Hursthouse, M. B.; Short, R. L. *Organometallics* **1987**, *6*, 2556. (c) Horton, A. D.; Frijns, J. H. G. *Angew. Chem., Int. Ed. Engl.* **1991**, *30*, 1152. (d) Ewen, J. A.; Elder, M. *J. Makromol. Chem., Macromol. Symp.* **1993**, *66*, 179.
(3) For reviews of stereocontrol in α-olefin polymerization, see: (a) Resconi, L.; Cavallo, L.; Fait, A.; Piemontesi, F. *Chem. Rev.* **2000**, *100*, 1253. (b) Coates, G. W. *Chem. Rev.* **2000**, *100*, 1253. (c) McKnight, A. L.; Waymouth, R. M. *Chem. Rev.* **1998**, *98*, 2587. (d) Alt, H. G.; Koppl, A. *Chem. Rev.* **2000**, *100*, 1205.

ridyl−amide-based group IV catalysts[7] were recently optimized via high-throughput technology to have an unprecedented combination of efficiency, molecular weight capability, and isotacticity in high-temperature propylene polymerization.[8−10] In addition, these catalysts have been applied in the high-volume preparation of olefin block copolymers through chain shuttling polymerization.[11,12]

In addition to outstanding polymerization performance, these catalysts have intriguing activation and polymerization mechanisms that seemingly generate new layers of complexity to trump any new level of understanding that is achieved. A salient structural feature of these complexes is a Hf−aryl bond that unexpectedly forms in the catalyst synthesis. This highly unusual feature of the ligand architecture has been linked to the high activity and stereoselectivity exhibited by these species. Despite complicated activation chemistry, many catalysts in this family produce propylene homopolymers with narrow molecular weight distributions. The stereocontrol mechanism of these chiral C_1-symmetric precursors has been the subject of a recent study.[8] The mechanism discussed therein is similar to that described for isospecific C_1-symmetric metallocenes possessing two diastereotopic coordination sites, in which monomer insertions occur exclusively at one face of the catalyst.[13]

We became especially interested in the activation mechanism after noting very broad molecular weight distributions (M_w/M_n, where M_w is the weight-average molecular weight and M_n is the number-average molecular weight) of ethylene−octene copolymers produced by this catalyst (Chart 1). The broad molecular weight distributions imply that these copolymers are not produced by a single active site. In fact, the gel permeation chromatography (GPC) traces are readily fit with two Schulz−Flory peaks, implying at least two distinct active sites. Deconvolution of one such trace shows that the copolymer depicted in Chart 1 comprises components with dramatically different molecular weights, containing 34 wt % of a low molecular weight fraction (M_w = 121 kg/mol) and 66 wt % at much higher molecular weight (M_w = 1140 kg/mol). We were therefore compelled to consider the possibility that the activation mechanism might have yet another layer of complexity. In an attempt to explain this behavior, we initiated a combined theoretical and experimental study to determine the identity of the active sites in copolymerizations using this class of catalysts.

Chart 1. GPC Trace of an Ethylene/Octene Copolymer Produced by **I** (Scheme 1) Activated by $[R_2MeNH][B(C_6F_5)_4]$[a]

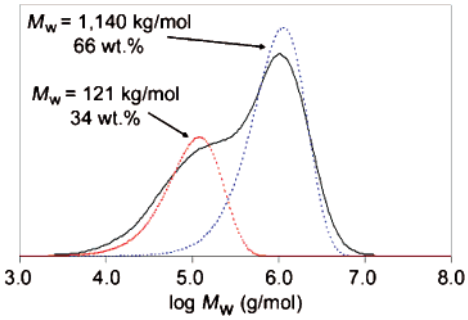

[a] The experimental trace and the deconvoluted bimodal composition are depicted.

Results and Discussion

The activation chemistry of the pyridyl−amide catalysts is complicated when Brønsted acids are used as cocatalysts (Scheme 1).[14] These species were shown to undergo an initial protonation of the aryl moiety when activated with anilinium borates, giving the hafnium dimethyl cation (**II**), which is inactive for polymerization. Long induction periods observed under these activation conditions have been attributed to slow conversion of **II** to **III** via rearylation and methane elimination. However, this activation chemistry does not explain the observed multisite behavior in ethylene/octene copolymerizations. Activation of the catalyst can be simplified by the use of Lewis acids such as tris(perfluorophenyl)borane ($B(C_6F_5)_3$), which lead to methide abstraction and direct generation of **III**. This route dramatically reduces the induction period in copolymerizations, but broad molecular weight distributions are still observed. Because the bimodal character is present regardless of whether the catalyst is activated by a protic or nonprotic activator, the bimodality cannot be readily explained by the activation chemistry shown in Scheme 1.

Having ruled out **II** as a possible active catalyst, we considered several possible modes by which multiple species could be formed. Eventually, we hypothesized that the observed multisite behavior is a result of modification of the catalyst by a single insertion of monomer into the hafnium−aryl bond leading to multiple catalyst behavior for copolymerizations. Insertions into metal−aryl bonds are fairly well-known in late metal systems but have little precedent for group IV systems. However, a stoichiometric insertion into a

(4) For reviews of late-metal catalysts for olefin polymerization, see: (a) Johnson, L. K.; Killian, C. M.; Brookhart, M. *J. Am. Chem. Soc.* **1995**, *117*, 6414. (b) Ittel, S. D.; Johnson, L. K.; Brookhart, M. *Chem. Rev.* **2000**, *100*, 1169. (c) Britovsek, G. J. P.; Gibson, V. C.; Kimberly, B. S.; Maddox, P. J.; McTavish, S. J.; Solan, G. A.; White, A. J. P.; Williams, D. J. *Chem. Commun.* **1998**, 849.
(5) For reviews of post-metallocene catalysts, see: (a) Gibson, V. C.; Spitzmesser, S. K. *Chem. Rev.* **2003**, *103*, 283−315. (b) Britovsek, G. J. P.; Gibson, V. C.; Wass, D. F. *Angew. Chem., Int. Ed.* **1999**, *38*, 429−447.
(6) For reviews of living olefin polymerization systems, see: (a) Domski, G. J.; Rose, J. M.; Coates, G. W.; Bolig, A. D.; Brookhart, M. *Prog. Polym. Sci.* **2007**, *32*, 30. (b) Coates, G. W.; Hustad, P. D.; Reinartz, S. *Angew. Chem., Int. Ed.* **2002**, *41*, 2236.
(7) Murray, R. E. PCT Int. Appl. WO1999001460 A1, 1999.
(8) Boussie, T. R.; Diamond, G. M.; Goh, C.; Hall, K. A.; LaPointe, A. M.; Leclerc, M. K.; Murphy, V.; Shoemaker, J. A. W.; Turner, H.; Rosen, R. K.; Stevens, J. C.; Alfano, F.; Busico, V.; Cipullo, R.; Talarico, G. *Angew. Chem., Int. Ed.* **2006**, *45* (20), 3278−3283.
(9) (a) Boussie, T. R.; Diamond, G. M.; Goh, C.; Hall, K. A.; LaPointe, A. M.; Leclerc, M. K.; Lund, C.; Murphy, V. U.S. Pat. Appl. 2006/0135722 A1, 2006. (b) Boussie, T. R.; Diamond, G. M.; Goh, C.; Hall, K. A.; LaPointe, A. M.; Leclerc, M. K.; Lund, C.; Murphy, V. U.S. Pat. 7,018,-949, 2006. (c) Boussie, T. R.; Diamond, G. M.; Goh, C.; LaPointe, A. M.; Leclerc, M. K.; Lund, C.; Murphy, V. U.S. Pat. 6,750,345, 2004. (d) Boussie, T. R.; Diamond, G. M.; Goh, C.; Hall, K. A.; LaPointe, A. M.; Leclerc, M. K.; Lund, C.; Murphy, V. U.S. Pat. 6,713,577, 2004. (e) Boussie, T. R.; Diamond, G. M.; Goh, C.; Hall, K. A.; LaPointe, A. M.; Leclerc, M. K.; Lund, C.; Murphy, V. U.S. Pat. 6,706,829, 2004. (f) Boussie, T. R.; Diamond, G. M.; Goh, C.; Hall, K. A.; LaPointe, A. M.; Leclerc, M. K.; Lund, C.; Murphy, V. PCT Int. Appl. WO 046249, 2002. (g) Boussie, T. R.; Diamond, G. M.; Goh, C.; Hall, K. A.; LaPointe, A. M.; Leclerc, M. K.; Lund, C.; Murphy, V. PCT Int. Appl. WO 038628, 2002.
(10) (a) Arriola, D. J.; Bokota, M.; Timmers, F. J. PCT Int. Appl. WO 026925 A1, 2004. (b) Coalter, J. N., III; Van Egmond, J. W.; Fouts, L. J., Jr.; Painter, R. B.; Vosejpka, P. C. PCT Int. Appl. WO 040195 A1, 2003. (c) Frazier, K. A.; Boone, H.; Vosejpka, P. C.; Stevens, J. C. U.S. Pat. Appl. 2004/0220050 A1, 2004. (d) Stevens, J. C.; Vanderlende, D. D. PCT Int. Appl. WO 040201 A1, 2003.
(11) Arriola, D. J.; Carnahan, E. M.; Hustad, P. D.; Kuhlman, R. L.; Wenzel, T. T. *Science (Washington, D.C.)* **2006**, *312* (5774), 714−719.
(12) Arriola, D. J.; Carnahan, E. M.; Cheung, Y. W.; Devore, D. D.; Graf, D. D.; Hustad, P. D.; Kuhlman, R. L.; Li Pi Shan, C.; Poon, B. C.; Roof, G. R.; Stevens, J. C.; Stirn, P. J.; Wenzel, T. T. U.S. Pat. Appl. 2005/090427, 2005.
(13) Miller, S. A.; Bercaw, J. E. *Organometallics* **2006**, *25* (15), 3576−3592.
(14) (a) Lapointe, A. M. Personal communication. (b) Macchioni, A.; Boone, H. W.; Busico, V.; Stevens, J. C.; Zuccaccia, C. *Abstracts of Papers*, 231st ACS National Meeting, Atlanta, GA, March 26−30, 2006; American Chemical Society: Washington, DC, 2006; BMGT-021.

Scheme 1. Catalyst Activation in the Presence of a Brønsted Acidic Cocatalyst

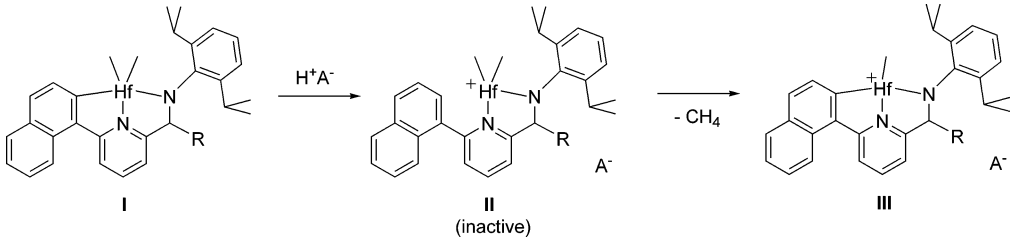

metal−aryl bond has been observed by Teuben and co-workers in a titanium bis(phenoxide) complex,[15] so the idea is not without precedent. Initially, we used density functional theory (DFT) calculations to provide insight into the possibility of monomer insertion into the hafnium−aryl bond to give a new type of active site.

Density Functional Theory Calculations. Scheme 2 depicts the proposed events relevant in polymerization of ethylene by **I**. The following simplifications are used to represent the ligand backbone: the pyridine ring is represented by "py", the 2-isopropylphenyl group by R, and the 2,6-diisopropylphenyl substituent by R′. DFT calculations were performed on the full catalyst to determine the relative enthalpies for these species and the relevant transition-state structures. The details of the calculations are provided in Computational Details. While much of the ligand backbone is coplanar, the chiral center at R does render the top and bottom faces inequivalent. Thus, there are two relevant starting positions, with alkyl "up" (*syn* to R on the backbone, **1a**) or alkyl "down" (*anti* to R, **1b**). The structures **1a**,**b** in the middle left of Scheme 2 are our beginning points. Going from left to right from **1a**/**1b** to **1a**′/**1b**′ depicts the conventional mechanism of consecutive ethylene insertions into the Hf−alkyl bond with the remainder of the structure acting as an innocent ligand. Due to the asymmetry of the catalyst, migratory insertion from top to bottom is not energetically equivalent to migratory insertion from bottom to top, so the two parallel pathways are considered. However, the chiral center at R is apparently far enough removed from the metal center of the "uninserted" complex to render the two pathways energetically similar.

The two precursor complexes, **1a**,**b**, with *n*-butyl groups representing polymer chains, differ in energy by 1.2 kcal/mol, with **1a** more stable. Two β-agostic intermediates were found for both **1a**,**b**, with the ethyl group bound to the β-carbon pointing either toward the naphthalene or the R′ group. In either **1a** or **1b**, the polymer chain preferentially points toward the smaller naphthyl group.[16] Each isomer has a strong agostic interaction that can be displaced by ethylene coordination. The energies of the reaction of ethylene binding of 9.8 (**2a**) and 8.1 kcal/mol (**2b**) are relatively large considering the loss of the stabilizing metal−agostic interaction. The binding is preferred on the bottom of the molecule (**2a**), opposite the bulky chiral center.[17] Continuing along the conventional insertion pathway in Scheme 2, olefin insertion occurs in a migratory fashion from either **2a** or **2b**. The relative transition state energies of **4a**‡ and **4b**‡ are similar despite significant differences in the complexation energies. The overall reaction energy is approximately 21 kcal/mol.

The key to our hypothesized mechanism is that the olefin complex **2a** (or **2b**) can insert an olefin into the Hf−aryl bond. Because of the proximity of the olefin to both the Hf−polymeryl and Hf−aryl bonds, this structure represents a common intermediate for the competing insertions, and the relative energies of the transition states ($\Delta\Delta H^{\ddagger}$) predicted by theory provide an excellent estimation of the relative rates. Remarkably, a lower barrier is found for insertion into the Hf−aryl bond than insertion into Hf−alkyl! Comparing transition states **3a**‡ and **4a**‡ reveals that insertion into the aryl bond is 0.4 kcal/mol lower when the olefin inserts trans to the R group. In fact, insertion into the Hf−aryl bond is even more favored (by 2.2 kcal/mol) when the olefin inserts cis (**3b**‡ vs **4b**‡). We also considered the possibility that chain growth continues between the metal and the aryl. However, comparing this "ring expansion" transition state to that leading to polymer chain growth (**8a**‡/**8b**‡, **9a**‡/**9b**‡) indicates that extending the Hf−CH_2CH_2−aryl linkage has a higher barrier by at least 15 kcal/mol. Thus, we can conclude that only one olefin inserts into the Hf−aryl bond.

The idea that insertion into the hafnium−aryl bond of **2a**,**b** could lead to an inactive species can be discounted by a simple kinetic consideration. This catalyst system typically generates productivities as high as 300 kg of polymer/g of Hf, equivalent to nearly two million insertions during its lifetime.[10c−d] Thus, the barrier ($\Delta G^{\ddagger}$) for any deactivation mechanism must be about 10 kcal/mol *higher* than that for propagation (at 130 °C). Therefore, if insertion into the Hf−aryl bond were a deactivation pathway, it would occur during the lifetime of the catalyst, *even if the barrier for insertion into the Hf−aryl bond were up to 10 kcal/mol higher*. Our calculations indicate the activation barrier for insertion into the Hf−aryl bond to be about 2 kcal/mol *lower* than that for propagation. It is highly unlikely that these calculations of relative activation barriers could be in error by so much (ca. 12 kcal/mol). Scheme 3 depicts our proposal for the activation process to the proposed active catalyst in ethylene polymerization.

The calculations here represent the polymer chain by an *n*-butyl group, but the conclusions also apply to the initial Hf−

(15) Gielens, E. E. C. G.; Dijkstra, T. W.; Berno, P.; Meetsma, A.; Hessen, B.; Teuben, J. H. *J. Organomet. Chem.* **1999**, *591*, 88−95.

(16) In calculations discussed further in this paper, if multiple rotamers are possible, only the lowest energy one is quoted; further details can be found in the Supporting Information.

(17) Interestingly, this binding is stronger than for many metallocene and constrained-geometry catalysts and, for **2a**, more closely resembles binding to late transition metal catalysts. Many group IV metallocenes have olefin binding energies in the 6−8 kcal/mol range relative to the β-agostic intermediate, and the inclusion of entropic effects at temperatures in the 100−200 °C range renders the olefin complex higher in energy than the initial metal−alkyl + olefin separated pair. Ultimately, this situation leads to activation parameters with low $\Delta H^{\ddagger}$ and large negative $\Delta S^{\ddagger}$. Late transition metal catalysts possess stronger olefin binding energies and the activation parameters with larger $\Delta H^{\ddagger}$ and smaller negative $\Delta S^{\ddagger}$ indicate the resting state is a bound olefin complex. In this case of the pyridyl−amide complexes **1**, the nature of the resting state is not known, but the large olefin binding energy is unusual for an early transition metal complex.

Scheme 2. General Features of the Potential Energy Surface for Ethylene Reacting with the Pyridyl−Amide Complex[a]

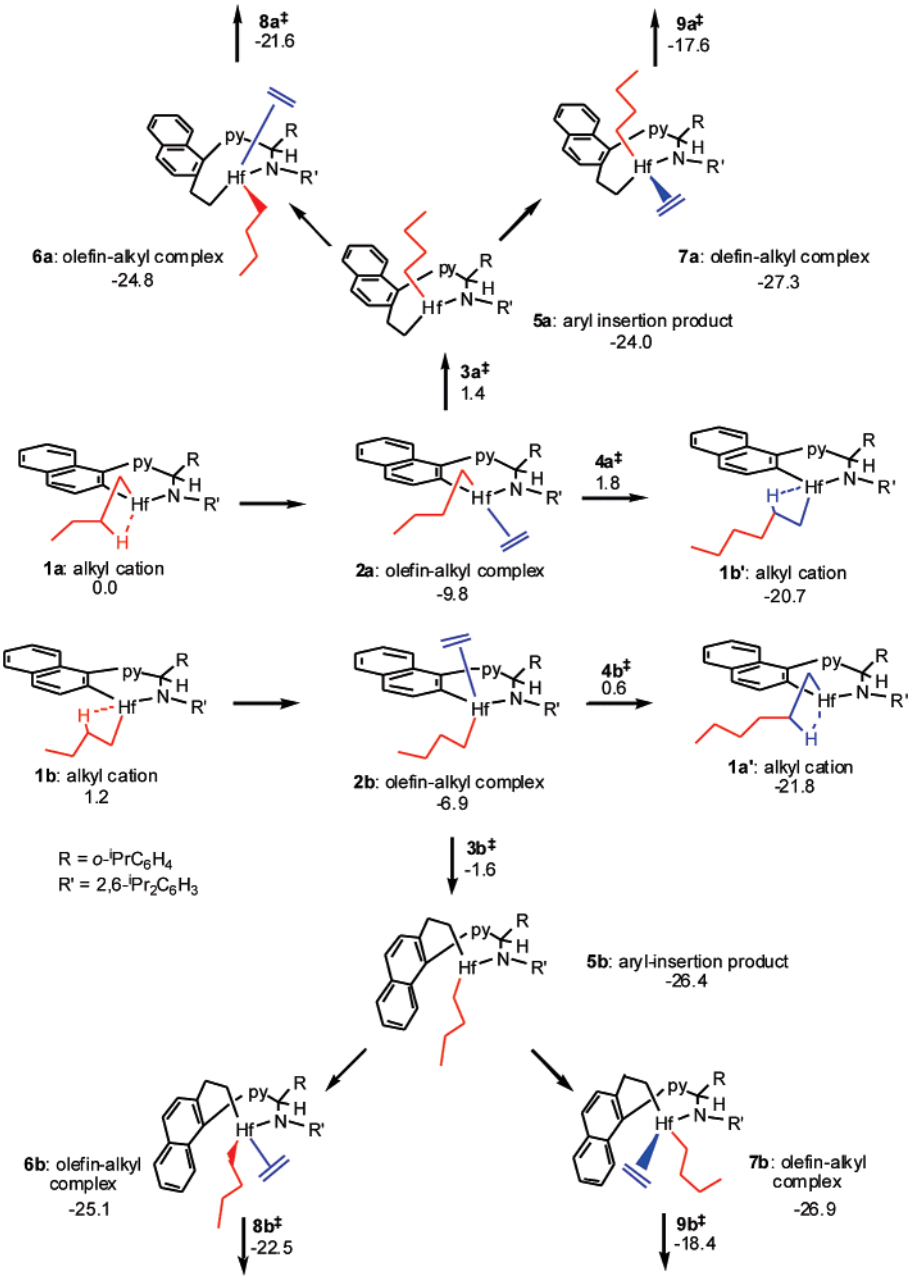

[a] All energies in kcal/mol at the B3LYP/6-311G** are relative to **1a**. Structures denoted with the double-daggers are transition states, and their energies are also relative to **1a**.

Scheme 3. Structures of the Catalyst Precursor, "Uninserted Complex", and "Monomer-Inserted Catalyst"

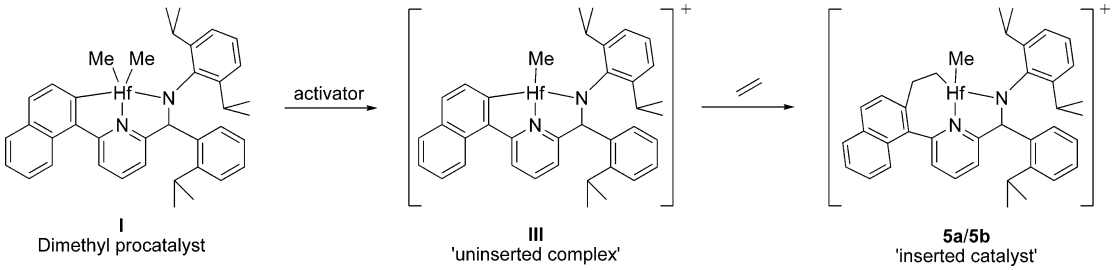

Me species. It is well-known[18,19] that insertions into M−Me bonds are often slower than insertions into M−polymeryl bonds, whereas insertion into this Hf−aryl bond is expected to be relatively insensitive to the Hf−alkyl. Thus, one might surmise that the $\Delta\Delta H^{\ddagger}$ values are even larger in favor of insertion into the Hf−aryl bond. In fact, the calculations confirm this. The $\Delta\Delta H^{\ddagger}$ values of 0.4 kcal/mol (**3a**‡/**4a**‡) and 2.2 kcal/mol (**3b**‡/**4b**‡) are increased to 3.0 and 7.4 kcal/mol, respectively, for the

(18) Landis, C. R.; Rosaaen, K. A.; Sillars, D. A. *J. Am. Chem. Soc.* **2003**, *125*, 1710.

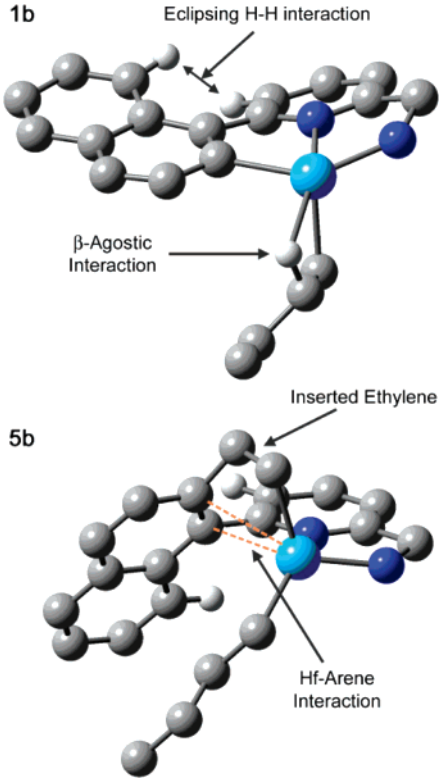

Figure 1. Calculated structures for one "uninserted" complex (**1b**) and for one of the products of insertion of ethylene into the Hf−naphthyl bond (**5b**). The substituted phenyl groups are removed for clarity. Hydrogens are not shown except to demonstrate the eclipsing H−H and β-agostic interactions in **1b**.

corresponding methyl complex. This is likely to be the more relevant comparison when **I** is used as the catalyst precursor. The reported 400-fold decrease in rate for a Zr−Me bond compared to a Zr−polymeryl[18] corresponds to a barrier difference of about 5 kcal/mol (at 130 °C), which agrees well with our calculated change in $\Delta\Delta H^{\ddagger}$.

The products of insertion into the Hf−aryl bond (**5a**,**b**) are also more stable than the products of polymeryl insertion (**1b′**/**1a′**) by 3−5 kcal/mol. One source of this stabilization is the elimination of an eclipsing H−H interaction (H−H distance = 1.9 Å) between hydrogens of the nearly coplanar naphthalene (16° dihedral angle) and pyridine rings in **1** (see Figure 1). Insertion into the Hf−aryl bond causes an increase in this dihedral angle to 62°, which not only alleviates this eclipse but also results in a favorable stabilizing hafnium−arene interaction. The ability of benzyl groups to facially coordinate in cationic catalysts is well-known.[20] In this case, the stabilization is reduced due to geometric constraints, but a stabilizing interaction is present nonetheless (calculated shortest Hf−C_{aryl} distances of 2.84 and 3.13 Å, Figure 1). However, one remarkable aspect of the monomer-inserted complexes is the lack of a β-agostic interaction usually observed in cationic group IV alkyl complexes. There does appear to be space for an agostic interaction, but despite repeated computational efforts, no structure with such an interaction could be located. Perhaps the additional electron donation from the aryl ring mitigates the need for agostic stabilization. For this reason, there is only one alkyl intermediate for **5a** and one for **5b**, whereas precursor **1** has two structures with the β-agostic interaction residing in the open coordination site.

We considered the possibility that the monomer-inserted species **5a**,**b** could isomerize. However, a transition state could not be located for the concerted ring flip, which is not surprising considering the strain imposed by a transition state with Hf, pyridine, aryl, and the two carbons of the Hf−CH_2CH_2−aryl linkage all copolanar, while the Hf−polymeryl wags to the opposite face. This is likely a high-energy process which does not occur to any significant extent at relevant polymerization conditions.

The olefin can approach the new catalysts (**5a**,**b**) either *anti* (**6a**,**b**) or *syn* (**7a**,**b**) to the monomer-inserted aryl moiety. In sharp contrast to **1a**,**b**, the olefin binding energies for **5a**,**b** are near zero, and the largest binding enthalpy found is only 3.3 kcal/mol (in **7a**). For **6b**, the binding enthalpy is actually endothermic! While DFT sometimes underestimates binding energies, the *difference* in binding behavior between **1** and **6**/**7** is quite significant.

Transition states were located for ethylene insertion into the olefin−alkyl complexes (**6**, **7**). Interestingly, the stronger olefin binding complexes on both sides (**7a**,**b**) have higher transition state energies, leading to larger barriers. The favored transition states (**8a**‡/**8b**‡) have the olefin approaching *anti* to the monomer-inserted aryl moiety. It appears that the stability of the transition state depends more on ethylene insertion *anti* to the newly created arylethyl substituent than any preference related to the chiral R moiety.

The difference between possible propagating species **1** and **5** is intriguing. Complex **1** has a strong β-agostic interaction, a relatively large olefin binding energy (−6.9 to −9.8 kcal/mol), and transition states on the two faces which are comparable in energy (differ by 1.2 kcal/mol). On the other hand, compounds **5a**,**b** have no β-agostic interaction, very weak olefin binding (+1.3 to −3.3 kcal/mol), and transition states on the two sides which differ by more than 4 kcal/mol. These data suggest that the monomer-inserted catalysts can easily chain wag or epimerize due to the lack of a β-agostic interaction and the reversibility of olefin binding. Thus, all insertions may occur from the face of the complex opposite the arylethyl substituent. This suggestion has implications for the highly isospecific α-olefin homopolymerization of this catalyst.[8−10] C_1-symmetric *ansa*-metallocenes sometimes have insertion rates competitive with or even faster than chain epimerization, most elegantly demonstrated by the formation of hemiisotactic polypropylene.[21] For this reason, formation of isotactic polypropylene using C_1-symmetric catalysts has generally been associated with slow polymerization kinetics. However, the relatively unimpeded chain epimerization in this catalyst may allow every insertion to occur in the same direction without slowing the overall polymerization kinetics.

Insertion into Hf−Aryl Bond and Copolymerization. The competitive insertion of ethylene into the Hf−polymeryl and

(19) (a) Herfert, N.; Fink, G. *Makromol. Chem., Macromol. Symp.* **1993**, *66*, 157. (b) Mehrkhodavandi, P.; Bonitatebus, P. J.; Schrock, R. R. *J. Am. Chem. Soc.* **2000**, *122*, 7841.

(20) For examples of η^2-benzyl interactions in zirconium cations, see: (a) Jordan, R. F.; LaPointe, R. E.; Bajgur, C. S.; Echols, S. F.; Willett, R. *J. Am. Chem. Soc.* **1987**, *109*, 4111−13. (b) Jordan, R. F.; LaPointe, R. E.; Baenziger, N.; Hinch, G. D. *Organometallics* **1990**, *9*, 1539−45.

(21) (a) Farina, M.; Di Silvestro, G.; Sozzani, P. *Macromolecules* **1993**, *26*, 946. (b) Resconi, L.; Guidotti, S.; Camurati, I.; Frabetti, R.; Focante, F.; Nifant'ev, I. E.; Laishevtsev, I. P. *Macromol. Chem. Phys.* **2005**, *206*, 1405.

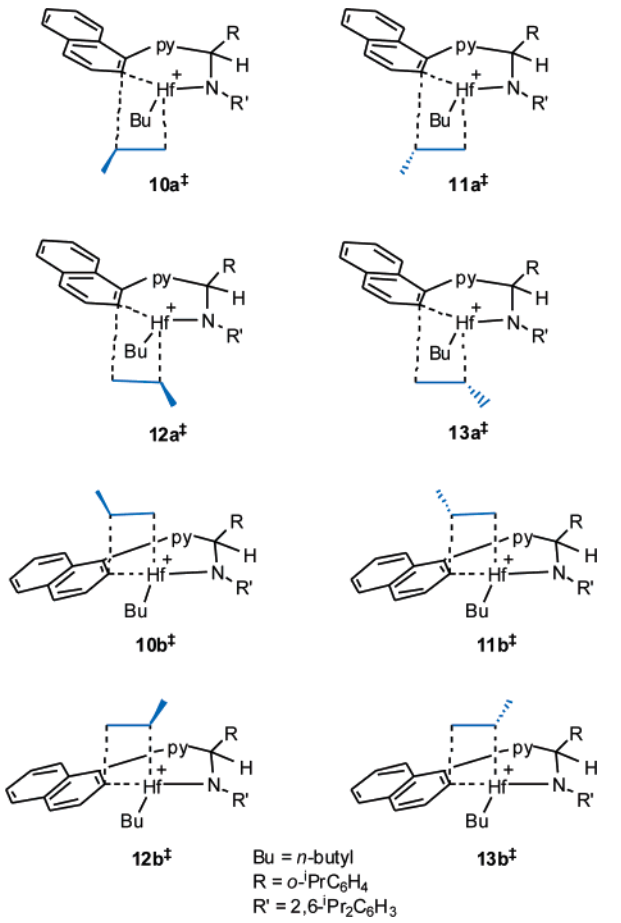

Figure 2. Possible transition states for propylene insertion into the Hf−aryl bond.

Hf−aryl bonds was discussed in detail in the previous section. In copolymerizations of ethylene and 1-octene, the two monomers presumably compete for insertion into the Hf−aryl bond, although it is well-known that the rate constant for α-olefin insertion into Hf−carbon bonds is slower. Hence, one would expect only a limited amount of "octene-inserted" catalyst to be formed relative to "ethylene-inserted" catalyst under typical copolymerization conditions where the concentration of ethylene is greater than octene.

Two ethylene-inserted and eight α-olefin-inserted catalysts can be formed (Figure 2) including facial selectivity, regioselectivity, and stereoselectivity. Due to the asymmetry imposed by the R substituent in the catalyst backbone, there are four transition states on the bottom of the catalyst (*anti* to the R group) in addition to four *syn* transition states. Hence, in ethylene/octene copolymerizations, 10 unique monomer-inserted catalysts, two from ethylene and eight from octene, can be formed.

Table 1 provides calculated transition state energies relative to **1a** for the olefin insertion into the Hf−aryl bond. As with typical propylene polymerizations, 2,1-insertions are disfavored and are not discussed further. However, 1,2-insertions, although higher in energy than those with ethylene, can compete to form additional monomer-inserted catalysts. It appears that the olefin approaching on the same side as the R substituent is favored, although one must recall that the starting alkyl cation, **1b**, is 1.2 kcal/mol higher than **1a**. The catalyst structures that are most likely to form to the greatest extent are **5b** (ethylene-inserted)

Table 1. Energies in kcal/mol Relative to **1a** for Transition States for Insertion into the Hf−Aryl Bond with Ethylene and Propylene[a]

compd	olefin *syn* to R	olefin *anti* to R
ethylene	−1.6 (**3b**‡)	1.4 (**3a**‡)
1,2-propylene	−0.6 (**10b**‡)	1.9 (**10a**‡)
1,2-propylene	0.8 (**11b**‡)	3.8 (**11a**‡)
2,1-propylene	7.8 (**12b**‡)	11.4 (**12a**‡)
2,1-propylene	3.3 (**13b**‡)	5.3 (**13a**‡)

[a] Possible regio- and stereoisomers of propylene are depicted in Figure 2.

and the products of the two 1,2-inserting olefin transition states *syn* to the R in the backbone (**10b**‡, **11b**‡). In the Supporting Information, further details on the structural and energetic information are provided.

Experimental Evidence for Insertion into the Hf−Aryl Bond. Following the DFT calculations, we set out to gather experimental evidence for this monomer modification hypothesis. We attempted to observe the active species in solution using NMR studies. As mentioned above, we have thus far been unable to effect stoichiometric generation of an monomer-inserted catalyst due to the complicated activation and polymerization kinetics. However, we sought to "filter" the spectrum to show only products relevant to ethylene reactions by employing doubly ^{13}C-labeled ethylene. The pyridyl−amide complex was activated with $B(C_6F_5)_3$ and reacted with ethylene (1.2 equiv) in an NMR tube at −80 °C. The initial spectra were recorded at −50 °C, and then the tube was warmed to −20 °C in the probe. After a few minutes and vigorous shaking of the NMR tube, the resonance corresponding to free ethylene at 123 ppm disappeared and two new peaks appeared at 35 and 69 ppm. We do not make any claims to determine a complex structure on the basis of these two ^{13}C resonances, but this experiment does demonstrate that ethylene has reacted in solution. The fact that only two new resonances are observed is consistent with a single ethylene insertion. Given that initiation with this cationic hafnium−methyl species is known to be much slower than propagation, it is reasonable to conclude that the insertion has not taken place into the hafnium−methyl bond, as this would likely lead to further insertions and produce multiple ^{13}C resonances.

To further characterize the nature of the observed reaction, the activated complex was hydrolyzed with aqueous base and the residue was analyzed by GC/MS. The residue showed primarily two products having $m/z = 512$ and $m/z = 540$ in a ca. 5:1 ratio. Although most of the residue corresponds to the original ligand, the species with $m/z = 540$ (ligand + $^{13}C_2H_4$) clearly demonstrates that a measurable fraction of the catalyst has appended an ethylene to the ligand in a reaction with only 1.2 equiv of monomer. Finally, ^{13}C NMR of this quenched reaction mixture shows strong resonances at 16.0 and 27.3 ppm, consistent with an ethyl group attached to a naphthyl substituent.[22]

To further elucidate this mechanism, we sought to isolate and fully characterize an olefin-appended ligand following polymerization. We used 4-methyl-1-pentene (4M1P) due to the ease of handling this liquid and the expected higher crystallinity imparted by the branched side chain compared to a straight-chain alkyl group such as octyl. A homopolymerization of 50

(22) Using ChemDraw Ultra, these chemical shifts are predicted at 14.9 and 26.2 ppm.

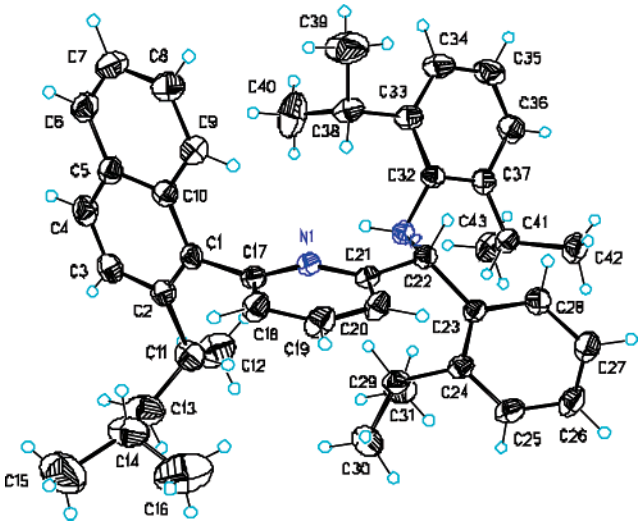

Figure 3. X-ray structure of the isolated 4M1P-inserted ligand residue, unambiguously demonstrating a monomer appended to the naphthyl carbon that was bound to the hafnium center.

equivalents of 4M1P was conducted with **I** activated by $B(C_6F_5)_3$, and the ligand residue was isolated following polymerization and quench. As in the ^{13}C-labeled ethylene polymerization described above, only a fraction of the monomer-inserted ligand was found in the residue. Species with *m*/*z* corresponding to 4M1P-inserted complexes made up around 30% of the ligand species. Interestingly, two separate compounds with this mass were observed by NMR following chromatography and successive recrystallizations. A single crystal of one of these species was analyzed by X-ray crystallography, and the structure demonstrates unambiguously that a 4M1P monomer is appended to the aryl at the carbon which was attached to hafnium (Figure 3). The two stereocenters in the molecule are of the same configuration (*R*,*R* or *S*,*S*). A comparison of the ^1H NMR spectra indicates that the second species is likely a diastereomer with (*R*,*S*) or (*S*,*R*) configuration, arising from a lack of selectivity of the initial insertion. It should be noted that the metal center is chiral; thus, the four diastereomers potentially generated by 1,2-insertion into the Hf−aryl bond are reduced to two in the ligand after quench.

During a copolymerization of ethylene and an α-olefin, the molecular weight distribution should be greater than two, as observed in Chart 1, if the copolymerization conditions produce a plurality of active catalysts and these catalysts produce polymer with different molecular weights. Our proposed activation scheme involves reaction of the catalyst with a monomer to form the active species. One would expect the population of these different sites, and therefore the polymers produced by them, to be a function of the relative concentrations of the two monomers present. Chart 2 shows GPC traces for ethylene/octene copolymers made at different reactor mole fractions of comonomer, f_2, where f_2 = [octene]/([ethylene] + [octene]). It is clear that the distribution between the two polymer fractions shifts as the mole fraction of octene is varied. The amount of the low and high molecular weight fractions (LMW and HMW, respectively) was estimated from the traces using a deconvolution routine (Table 2). More of the high molecular weight polymer is formed as the monomer composition changes to a more octene-rich environment, moving from 41 to 83 wt % HMW across the investigated composition range. We

Chart 2. GPC Traces of Ethylene/Octene Copolymers Produced at Different Reactor Mole Fractions of Octene (f_2)

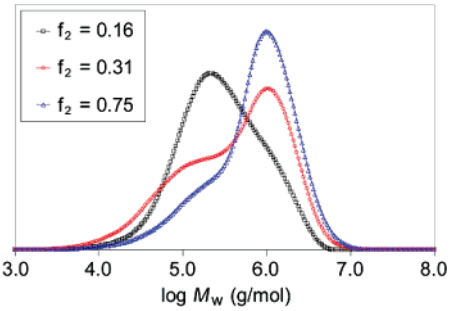

therefore tentatively conclude that the higher molecular weight fraction is produced by an octene-inserted catalyst(s), while an ethylene-inserted species forms polymer with lower molecular weight. Generally, molecular weights systematically decrease in copolymerizations when α-olefin concentration is increased, due to more facile chain transfer following α-olefin incorporation.

The rates of formation of the ethylene- and octene-inserted catalysts change as one varies the mole fraction of octene. The rate constant for ethylene insertion is larger than that for octene as ethylene almost always has a faster rate of insertion than α-olefins.[23] In agreement with this, Table 1 shows the ethylene insertion transition state to be lower. Given the intermediate level of comonomer with an octene mole fraction of 0.31 (red line in Chart 2), both the rate constant for formation of the octene-inserted catalyst and the octene concentration are lower. Thus, less of the octene-inserted catalysts must be formed, yet the amount of polymer apparently produced by this species is greater. If our assumptions about the nature of the catalyst sites are correct, these data suggest that the octene-inserted catalyst(s) are significantly more active than the ethylene-inserted catalyst(s).[24]

The bimodality of ethylene/octene copolymers appears to indicate two discrete catalyst species. However, the DFT calculations and the 4M1P result described above suggest that more than two types of sites are present. The apparent bimodal distribution indicates one of two possibilities: (a) Only one each of an ethylene- and octene-inserted catalyst is formed; (b) multiple ethylene- and/or octene-inserted species are formed but the molecular weight capability is nearly independent of selectivity of the first insertion, thus approximating dual-site behavior.

Notably, the deconvolution yields a better fit by removing the Schulz−Flory constraint on the two components, giving broader distributions for the LMW (M_w/M_n = 3.15) and HMW fractions (M_w/M_n = 2.31). These deconvolutions are compared in Chart 3.[25] Not surprisingly, even ethylene homopolymer from this catalyst system displays a broad molecular weight distribution (M_w/M_n = 4.5). DFT calculations favor formation of one ethylene-inserted catalyst (**5b**), but it is important to remember that these GPC traces are composites of the amount of each

(23) For a catalyst system claimed to exhibit a higher reactivity for α-olefins than for ethylene, see: Irwin, L. J.; Reibenspies, J. H.; Miller, S. A. *J. Am. Chem. Soc.* **2004**, *126*, 16716−16717.
(24) The trend in catalyst activity in Table 2 is not clear, but we consider analysis of the GPC data to be more reliable.
(25) Additional details of the GPC deconvolutions are given in the Supporting Information.

Table 2. Experimental Data Including Deconvolutions of the GPC Traces for Ethylene/Octene Copolymers from **I**/[R_2MeNH][$B(C_6F_5)_4$][a]

sample	activity (g mmol^{-1} h^{-1} bar^{-1})	f_2	M_w (tot.) (kg/mol)	M_w/M_n (tot.)	wt % (LMW)	M_w (LMW) (kg/mol)	wt % (HMW)	M_w (HMW) (kg/mol)
1	4400	0.16	532	3.71	59	194	41	936
2	2000	0.31	875	7.35	34	121	66	1140
3	3300	0.75	1180	4.81	17	133	83	1190

[a] The component distributions are constrained to have $M_w/M_n = 2$.

Chart 3. Deconvolutions of the GPC Trace of the Ethylene/Octene Copolymer from Sample 2 with (a) Schulz−Flory Constrained Distributions and (b) No Constraint on the M_w/M_n of Each Component

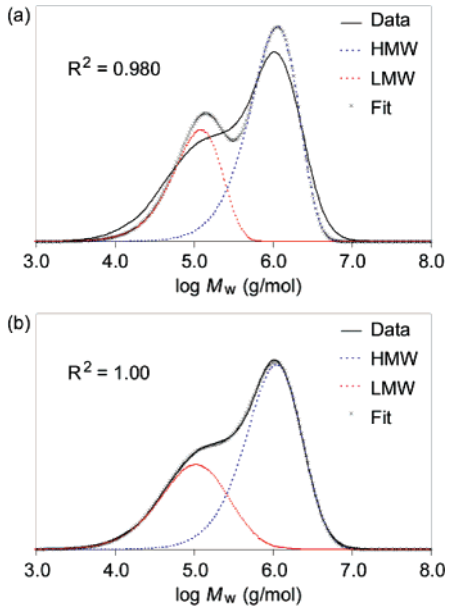

active site formed and their respective efficiencies. In contrast, poly(α-olefins) from this procatalyst normally have narrow molecular weight and composition distributions, but samples prepared with related pyridyl−amide complexes also show multisite characteristics.[26] Upon closer inspection of the GPC deconvolutions, we find that much better fits are obtained by unconstraining the M_w/M_n of the two components. Therefore, the latter explanation of multiple ethylene- and octene-inserted active species is more consistent with our predictions and observations. Scheme 4 summarizes our current proposal for the formation of active sites in ethylene/α-olefin copolymerizations with these pyridyl−amide complexes.[27]

Conclusions

Pyridyl−amide catalysts possessing a Hf−naphthyl bond (**I**) undergo an unusual and slow activation process with Brönsted acid activators. We propose that the initially generated complexes (**III** or **1**) are not the principal active species for polymerization. Rather, further modification of the ligand structure by insertion of an olefin into the Hf−aryl bond leads to the highly active polymerization catalysts. DFT calculations show that olefin insertion into the Hf−aryl bond of the pyridyl−amide catalyst **1** is at least competitive with insertion into the Hf−polymeryl bond and has a significantly lower barrier in most cases. These calculations also show the drastic difference between structural and energetic features of **1** compared to **5**. The uninserted complex, **1**, has strong β-agostic interactions, larger olefin binding energies, is two-sited, and possesses transition state energies that are similar on the two sides. In sharp contrast, **5** has no β-agostic interaction, very weak binding energies, possesses only one site with easy epimerization of the chain, and the transition state energies on two sides differ by more 4 kcal/mol with olefin preferring to approach *anti* to the olefin-inserted aryl moiety.

In ethylene−octene polymerizations, 10 unique olefin inserted catalysts are possible, but likely one ethylene-inserted and two octene-inserted catalysts are formed. ^{13}C-labeled ethylene and 4M1P quench experiments using GC/MS indicate insertion of the monomer into the Hf−aryl bond. However, only a fraction (20−30%) of monomer-inserted ligand is recovered, probably because a small percentage of monomer-inserted species polymerizes the remainder of the limited monomer present. This phenomenon complicates isolation or complete characterization of monomer-inserted catalysts. However, a crystal structure of a 4-methylpentyl-appended ligand following the quench shows unequivocally that the monomer inserted in a 1,2-fashion and NMR suggests that a second species was also a 1,2-inserted diastereomer.

Experimentally, it was shown that the bimodal nature of ethylene/octene copolymers changes as a function of the reactor mole fraction octene, f_2. At low f_2, the polymer contains more of a low molecular weight species, but as the f_2 is increased, the distribution shifts and more of a high molecular weight polymer is formed. This correlation of the bimodal distribution to reactor composition, which is related to the population of catalyst active sites, is consistent with our proposed mechanism of catalyst modification by monomer insertion into the hafnium−aryl bond.

This olefin polymerization catalyst system is truly in a class of its own, both in terms of polymerization performance and mechanistic complexity. While this work represents an advance in understanding, the mechanistic depths may not yet be fully explored, and we anticipate that further studies will continue to provide rich new insights.[28]

(26) For examples of poly(α-olefins) from related pyridylamido procatalysts with broad molecular weight distributions and multiple melting peaks, see refs 10c,d.

(27) Several other potential active species have been considered to explain these homopolymerization results. One possibility involves β-elimination of the aryl−ethyl to give a styryl species followed by reinsertion in a 2,1-fashion to give a benzylic ligand. The same site could also result from hydrogenolysis of the aryl−ethyl moiety followed by C−H activation at the benzylic carbon (this proposed mechanism was inspired by a reviewer's comments). We are investigating these possibilities, but preliminary DFT calculations and experimental work do not support them.

(28) Note added in proof: Coates reported an achiral, C_s-symmetric pyridyl−amide catalyst that forms isotactic polypropylene. This observation supports our proposed mechanism of ligand modification by monomer. Domski, G. J.; Lobkovsky, E. B.; Coates, G. W. *Macromolecules* **2007**, *40*, ASAP article.

Scheme 4. Catalyst Activation through Insertion of Ethylene and α-Olefin into the Hf−Aryl Bond

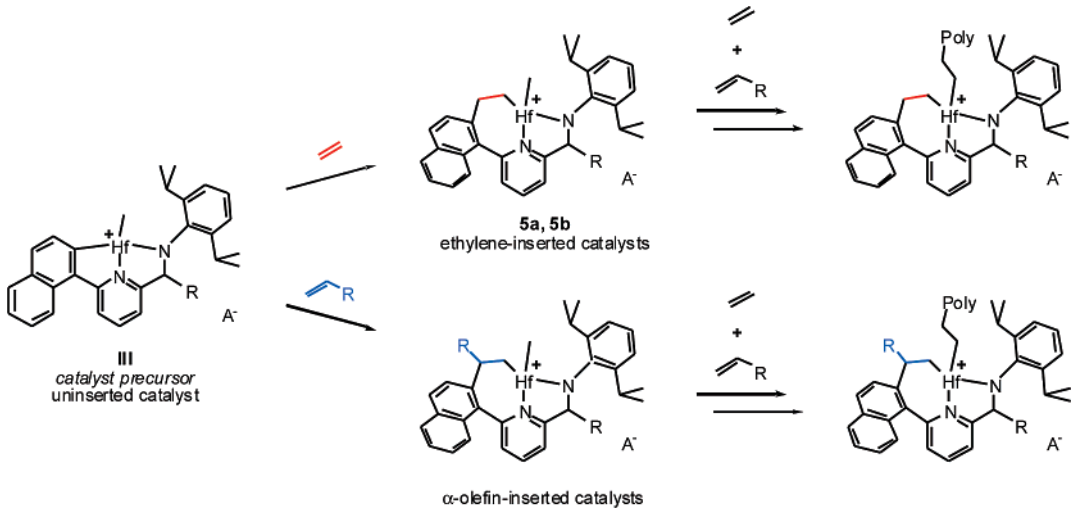

Experimental Section

Computational Details. Calculations were performed with the Gaussian03 program.[29] The catalysts considered were the methyl cation and the butyl cation. In this paper, results are quoted using a catalyst possessing an *n*-butyl group representative of the polymeryl chain, but qualitatively similar results are seen for the hafnium methyl catalyst, which is probably more demonstrative of the initiation reaction. Data for the reactions of both catalyst precursors are presented in the Supporting Information. In addition, the main thrust of this paper is a comparison of relative transition state energies, $\Delta\Delta H^{\ddagger}$, and it has been shown that the counterion is generally in the outer sphere in the transition state.[30] Geometry optimizations were performed using the B3LYP method[31] and the LANL2DZ basis set[32] (denoted BS-I), and structures were reoptimized at the B3LYP level using a basis set with LANL2DZ on hafnium and 6-31G*(5d)[33] on the remaining atoms (denoted BS-II). Using these geometries, single point energies were performed with the B3LYP method and LANL2DZ on hafnium and 6-311G**[34] on the remaining atoms (denoted BS-III). Further single point calculations utilizing the geometries from B3LYP/BS-II were performed using second-order Møller−Plesset perturbation theory[35] (MP2/BS-II). In this paper, enthalpies are quoted at the B3LYP/BS-III level utilizing the B3LYP/BS-II geometries, but qualitatively, the results (i.e., the differences in transition state energies, $\Delta\Delta H^{\ddagger}$) are the same at all levels of theory. Tables of energies and geometries are provided in the Supporting Information.

General Procedure for Batch Polymerizations. A 1 gallon AE autoclave was purged at high temperature with N_2. A mixed hydrocarbon solvent Isopar E was added, and the reactor was heated to 120 °C. 1-Octene and hydrogen were added batchwise to the reactor and were not regulated during the run. Hydrogen was required to produce polymers with molecular weights low enough to be routinely measured by gel permeation chromatography. The reactor was pressurized with ethylene (450 psi). Solutions of the catalyst, bis(hydrogenated tallowalkyl)methylammonium tetrakis(pentafluorophenyl)borate cocatalyst ($[R_2MeNH][B(C_6F_5)_4]$) (1.2 equiv), and modified methylalumoxane (MMAO) scavenger (5:1 Al−Hf) were mixed and then added to the reactor using a flush of high-pressure Isopar E. Polymer yield was kept low to minimize monomer composition drift during the experiment. After 10 min, reactor contents were dumped into a resin kettle and mixed with Irganox 1010/Irgafos 168 stabilizer mixture (1 g). The polymer was recovered by evaporating the majority of the solvent at room temperature and then dried further in a vacuum oven overnight at 90 °C. Following the run, the reactor was hot-flushed with Isopar E to prevent polymer contamination from run to run.

NMR Studies of I/$B(C_6F_5)_3$ and $^{13}C_2H_4$. A solution of **I** (37.6 mg, 52 μmol) in toluene-d_8 (2 mL) was added to a solution of $B(C_6F_5)_3$ (29.4 mg, 57 μmol) in toluene-d_8 (0.5 mL). After about 1 min, 1.2 mL of this solution was transferred to an NMR tube with a septum top. The tube was cooled to −80 °C, and 1.2 equiv of $^{13}C_2H_4$ gas (0.7 mL, 29 umol) was added via syringe. The tube was shaken and then transferred to the NMR probe, temperature-controlled at −50 °C.

After the NMR studies, the reaction mixture was quenched with aqueous base. The organic fraction was separated and analyzed by GC/MS and then transferred back to an NMR tube for ^{13}C NMR of the ligand.

Isolation of 4-Methyl-1-pentene-Appended Ligand Residue. Under nitrogen atmosphere in a drybox, a solution of **I** (2.05 g, 2.85 mmol) in toluene (40 mL) at room temperature was treated with $B(C_6F_5)_3$ (2.89 g, 5.64 mmol, 2 equiv) in toluene (20 mL). After being stirred for 5 min, 4-methyl-1-pentene (4M1P) (18.0 mL, 142 mmol, 50 equiv) was added to the solution, resulting in a sizable immediate exotherm and a very viscous solution that quickly gelled completely. The jar was removed from the drybox, and the reaction was quenched with copious methanol. The precipitated polymer was collected on a frit and washed with methanol, giving white solid poly(4M1P).

The combined filtrates were analyzed by GC-MS, which revealed a mixture of compounds including several peaks corresponding to 4M1P insertion products (*m*/*z* 596). After removal of methanol in vacuo, the ligand residue was purified by flash chromatography using a hexanes/

(29) Frisch, M. J.; et al. *Gaussian 03*, revision C.02; Gaussian, Inc.: Wallingford, CT, 2004. For the complete reference, see the Supporting Information.
(30) Landis, C. R.; Rosaaen, K. A.; Uddin, J. *J. Am. Chem. Soc.* **2002**, *124*, 12062.
(31) (a) Becke, A. D. *J. Chem. Phys.* **1993**, *98*, 5648. (b) Lee, C.; Yang, W.; Parr, R. G. *Phys. Rev B* **1988**, *37*, 785. (c) Miehlich, B.; Savin, A.; Stoll, H.; Preuss, H. *Chem. Phys. Lett.* **1989**, *157*, 200.
(32) (a) Dunning, T. H., Jr.; Hay, P. J. In *Modern Theoretical Chemistry*; Schaefer, H. F., III, Ed.; Plenum: New York, 1976; Vol 3, 1. (b) Hay, P. J.; Wadt, W. R. *J. Chem. Phys.* **1985**, *82*, 270. (c) Wadt, W. R; Hay, P. J. *J. Chem. Phys.* **1985**, *82*, 284. (d) Hay, P. J.; Wadt, W. R. *J. Chem. Phys.* **1985**, *82*, 299.
(33) (a) Ditchfield, R.; Hehre, W. J.; Pople, J. A. *J. Chem. Phys.* **1971**, *54*, 724. (b) Hehre, W. J.; Ditchfield, R.; Pople, J. A. *J. Chem. Phys.* **1972**, *56*, 2257. (c) Gordon, M. S. *Chem. Phys. Lett.* **1980**, *76*, 163.
(34) (a) McLean, A. D.; Chandler, G. S. *J. Chem. Phys.* **1980**, *72*, 5639. (b) Krishnan, R.; Binkley, J. S.; Seeger, R.; Pople, J. A. *J. Chem. Phys.* **1980**, *72*, 650.
(35) (a) Møller, C.; Plesset, M. S. *Phys. Rev.* **1934**, *46*, 618. (b) Head-Gordon, M.; Pople, J. A.; Frisch, M. J. *Chem. Phys. Lett.* **1988**, *153*, 503. (c) Frisch, M. J.; Head-Gordon, M.; Pople, J. A. *Chem. Phys. Lett.* **1990**, *166*, 275. (d) Frisch, M. J.; Head-Gordon, M.; Pople, J. A. *Chem. Phys. Lett.* **1990**, *166*, 281. (e) Head-Gordon, M.; Head-Gordon, T. *Chem. Phys. Lett.* **1994**, *220*, 122. (f) Saebo, S.; Almlof, J. *Chem. Phys. Lett.* **1989**, *154*, 83.

ethyl acetate stepwise solvent gradient. Selected fractions were combined to give a mixture of the free ligand (*m*/*z* 512) and the 4M1P−ligand (*m*/*z* = 596) in a 4:1 ratio. The residue was taken up in hot methanol and cooled slowly, which facilitated crystallization of a portion of the free ligand. Following several successive crystallizations, two different species with *m*/*z* 596 were isolated, giving approximately 20 mg of each compound. These species were characterized by ^{1}H NMR and COSY spectroscopy. A suitable crystal of one of the isomers was used to obtain an X-ray crystal structure, which unambiguously confirmed that the compound was the product of a primary insertion of 4MP1 into the hafnium−naphthyl bond. Full details of the X-ray analysis and NMR characterization of these species are listed in the Supporting Information.

Acknowledgment. We thank Khalil Abboud for solving the X-ray structure of the 4M1P-appended ligand, Brandon Garcia and Patricia Easter for performing batch reactor polymerization experiments, and Mike Nelson for conducting GPC analyses. Jim Stevens, Ted Carnahan, Jack Coalter, Paul Vosejpka, Alceo Macchioni, and Vincenzo Busico are also thanked for many helpful discussions.

Supporting Information Available: Additional computational data, energies, Cartesian coordinates of the structures, further experimental details of the copolymers, NMR characterization of the 4M1P-inserted ligand, GPC deconvolutions, and complete ref 29. This material is available free of charge via the Internet at http://pubs.acs.org.

JA070718F